Progress In Electromagnetics Research, Vol. 123, 299–320, 2012

GRADUAL THINNING SYNTHESIS FOR LINEAR ARRAY BASED ON ITERATIVE FOURIER TECHNIQUES

X.-K. Wang*, Y.-C. Jiao, and Y.-Y. Tan

National Key Laboratory of Antennas and Microwave Technology, Xidian University, No. 2, South Taibai Road, Xi'an, Shaanxi 710071, China

Abstract—In this paper, a modified iterative fourier technique (MIFT) for thinning uniformly spaced linear arrays featuring a minimum sidelobe level as well as narrow beam is presented. Since IFT is a thinning procedure which has to be performed many trial times with different initial element distributions to get the optimum solution, it is, to some extent, time consuming. Moreover, in each trial of IFT, the number of iterations is usually low, which makes the method tend to be trapped in local solution even with a large number of trials. Therefore, the similar procedures for both MIFT and IFT are to derive the element excitations from the prescribed array factor using successive forward and backward Fourier transforms, and array thinning is accomplished by setting the amplitudes of a predetermined number of the largest element excitations to unity while the others to zero during each iteration cycle. Furthermore, in MIFT, based on the idea of gradual thinning which is inspired by perturbation theory, an adaptively changed fill factor is proposed to modify IFT with the purpose of accelerating computational speed and facilitating convergence. The immediate result caused by this modified fill factor can be embodied in two points. One point is that unlike the random number of iterations contained in different trials of IFT, the number of iterations in all trials of MIFT is a fixed value and only predetermined by the array inherent features (symmetrical or asymmetrical) and fill factor. Therefore, sufficient iterations are ensured in each trial to effectively help the algorithm avoid trapping. The other point is that when MIFT is performed, the array elements are gradually truncated, which maintains the most useful element excitations while maximally excludes the bad excitations, so that the optimum solution

Received 9 October 2011, Accepted 20 December 2011, Scheduled 29 December 2011

* Corresponding author: Xin-Kuan Wang (xkwang@stu.xidian.edu.cn).

could be obtained through only a small number of trials and thereby substantially save computational cost. The effectiveness of MIFT will be demonstrated for various linear arrays and compared with the published reports.

1. INTRODUCTION

One of the most typical problems involving antenna arrays is the design of a set of feeding values that must be applied to the ports of an array in order to obtain a radiation pattern complying with certain specifications. This problem is usually referred to as synthesis [1]. Various techniques have been developed for array synthesis, such as the modified polynomial method [2], the general method based on an iterative process [3], particle swarm optimization methods (PSO) [4–11], genetic algorithms (GA) [12, 13], differential evolution(DE) approaches [14–16], simulated annealing techniques [17], hybrid methods [18–20], ant colony optimization ways (ACO) [21], etc. [22–25].

Array thinning is one important way of synthesis through which we expect not only to lower the sidelobe level (SLL) but also to reduce the number of array elements and thereby cut down cost substantially. In addition, the uniformly excited array is desired to minimize the complexity in designing a feed network even though it may suffer from high sidelobe level. To further lower SLL, array thinning is also a good way to make a compromise between low SLL and narrow beam.

Although different algorithms, from GA, PSO, ACO to various other methods, have been used for thinned array synthesis [26–32], the common characteristic of these methods is that the number of array elements should be small. For the array which contains plenty of elements, the computation time will be considerably increased by using above methods.

In recent years, a high efficiency method named iterative Fourier technique (IFT) has been presented by Keizer for thinning uniformly excited periodic arrays [33–35]. The method is actually a version of the alternating projection techniques [36, 37]. It derives the element excitations from the prescribed array factor using successive forward and backward Fourier transformations. Array thinning is accomplished by setting the amplitudes of the largest element excitations to unity and the others to zero in each iteration cycle [33].

Although IFT had been proved very efficient for linear array synthesis [33], the generally small number of iterations in each trial may make the method trap in local solutions. In addition, the method has to be performed many trial times with different starting

points to get the optimum solution, which is to some extent time consuming. Therefore, in this paper, a modified Fourier technique (MIFT) is presented to accelerate computational speed and facilitate convergence. The most notable difference between IFT and MIFT is that an adaptively changed fill factor f is introduced. To depict this modified version, we suppose that f_0 is the object fill factor that has an expected constant value. Therefore, in each trial of MIFT, f is adaptively decreased from a value approaching 1.0 to the object value f_0 with the increment of iterations. More clearly, it means that in one arbitrary trial, different iteration cycles correspond to different fill factors and that when the iteration within that trial is terminated, f will arrive at the object fill factor f_0. It obviously differs from IFT of which the fill factor has a constant value of f_0 for all the iteration cycles.

To demonstrate the good features of MIFT, we further suppose γ to represent the total number of iterations in each trial of IFT or MIFT. Because the quality of synthesis results largely depend on γ, a suitable value of γ is generally very useful for getting good solutions. However, in IFT, γ is mainly determined by the initial element distributions and the requirement peak sidelobe level (RPSL), and the bad initial distributions or unsuitable RPSL would make γ a low value (always less than 10) so that the iteration is quickly broken off, and the algorithm may be trapped in local solutions. Whereas in MIFT, γ is solely determined by the array itself and the object fill factor f_0, thus a suitable and fixed value of γ is predetermined for all trials, which could excellently help to facilitate convergence of the algorithm.

Then MIFT is performed for thinning various linear arrays. The synthesis results show that for small and medium size arrays, the method could effectively get the possible optimum solution but save computational cost many times or even more than IFT, GA and ACO. However, if the array is massively truncated, the mainlobe widening will be un-neglected using MIFT, so we further modify MIFT in order to maintain narrow beam as well as low sidelobe level. The synthesis results also satisfy our requirement with high efficiency.

2. MODIFIED ITERATIVE FOURIER TECHNIQUES

The IFT is a high efficiency method for thinned array synthesis as shown in the report [33]. However, as related above, the method is apt to trap, and the algorithm's convergence speed could also be further accelerated. So in this section, we propose a modified version to realize global convergence and accelerate computational speed.

As a start, we suppose a linear array with M elements equally

spaced at distance d, and the array's far field pattern $F(u)$ can be written as the product of the embedded element pattern EF and the array factor AF [33],

$$F(u) = EF(u)AF(u) \tag{1}$$

$$AF(u) = \sum_{m=0}^{M-1} A_m e^{jkmdu} \tag{2}$$

where $A_m\,(m = 1, 2 \ldots, M)$ is the complex excitation of the mth element, k the wave number, λ the wavelength, d the element spacing, $u = \sin\theta$ the direction cosine, and θ the pattern angle measured from broadside of the array. Equation (2) represents a finite Fourier series which relates the element excitation coefficients $\{A_m\}$ of the linear array to their AF through a discrete inverse Fourier transform (IDFT). A discrete direct Fourier transform (DFT) applied on AF will yield the element excitation coefficients $\{A_m\}$ [33].

According to Keizer's IFT method, the inverse fast Fourier transform (IFFT) and forward fast Fourier transform (FFT) were repeatedly implemented to get AF and $\{A_m\}$, respectively. If there is any sampling point in sidelobe region whose SLL exceeds RPSL, the method will forcefully make the SLL below RPSL. Array thinning is accomplished by setting the $M \cdot f_0$ samples of $\{A_m\}$ which have the largest amplitudes equal to unity and others to zero in each iteration cycle.

Furthermore, in MIFT, based on the idea of gradual thinning which is inspired by perturbation theory, an adaptively changed fill factor f is introduced into above procedures so that in each iteration cycle of one arbitrary trial, the element excitations are gradually truncated, which makes the most useful element excitations that contribute to the sidelobe level retained, and thereby we expect to find the optimum solution through only a small number of trials. The detailed step of MIFT proceeds as follows.

1) Randomly initialize the element excitations $A_m\,(m = 1, 2 \ldots, M)$ with probability of 0.9 equal to one (turned on) and the rest equal to zero.
2) Fourier transform is applied to the element excitations $\{A_m\}$ with K point IFFT to arrive the array factor AF consisting of K samples with $K > M$ by applying zero padding.
3) Match the sidelobe region of AF to the sidelobe requirement and make the AF values in the sidelobe region not exceed the RPSL unchanged. The AF values in the mainlobe region are unchanged, too.
4) Compute $\{A_m\}$ for the matched AF using K point forward FFT;

5) Truncate the K samples of $\{A_m\}$ to M samples associated with the array elements.
6) Set the $M \cdot f$ samples of $\{A_m\}$ which have the largest amplitudes equal to one and others to zero, where f is the adaptively changed fill factor whose initial value approaches 1.0.
7) Decrease f with step size of α, i.e., $f = f - \alpha$, where α is a positive value which makes only one element for asymmetrical array and two elements for symmetrical array to be truncated in each iteration cycle.
8) Repeat step 2) through step 7) until f arrives at the object fill factor f_0, then the iteration within that trial is terminated;
9) Step into the next trial: repeat step 1) through step 8) until the specified number of trials is reached.

Comparing the two methods, it could be seen that MIFT has the same steps as IFT from step 2) to step 6) [33, 34]. It differs from IFT mainly in three aspects.

The first aspect is that unlike the equal 0/1 probability for all the initial element distributions in IFT, the initial element distributions are set equal to one with probability of 0.9 and to zero with probability of 0.1 in MIFT. It means that the array is approaching full. The second, also the most important aspect, is that in IFT, different iteration cycles have the same fill factor f_0 while in MIFT, the fill factor is adaptively changed with the increment of iteration cycles. The third aspect is that in each trial of IFT, different initial element distributions make the value of γ a random one and that the algorithm is performed iteratively until the same element distributions are obtained by adjacent iterations. However, among different trials of MIFT, γ is a fixed value, and the algorithm is broken off just when the object fill factor f_0 is arrived.

The advantage of MIFT could be explained by perturbation theory. Suppose a system Φ which is partly deviated from the original system Φ_0. For simplicity, we suppose that ε_0 and ε respectively represent the solution of Φ_0 and Φ. According to perturbation theory, ε could be treated as the tiny disturbance to ε_0 and written as.

$$\varepsilon = \varepsilon_0 + \delta \tag{3}$$

We can see that ε consists of two parts: the first part, ε_0, is the main part of ε; the secondary part, δ, represents the part of solution produced by the influence of environment input. Therefore, the majority of inherent features of Φ_0 could be inherited to Φ.

Accordingly, in the first step of MIFT, a near-filled initial array would be enjoyed because it has higher directivity than the sparse-filled

array (If the array is filled, the obtained results in all trials would be identical). Then, through gradual thinning, we expect to obtain an array which could succeed to the high directivity of the initial array as much as possible.

Moreover, since the difference between different trials lies in the fact that the initial element distributions are different, the initial array and final solution are different, too. Therefore, both IFT and MIFT need several independent trials among which the optimum solution is selected. However, in each iteration cycle of IFT, the number of truncated elements is $M \cdot (1 - f_0)$, and this massively turned off element illuminations may cause some very useful elements removed and thereby severe deteriorate the synthesis solution. So in each trial of MIFT, through an adaptively changed fill factor, only one element for an asymmetrical array and two elements for a symmetrical array (the two elements are symmetrical with their center at the origin) which have the lowest amplitudes are truncated in each iteration cycle. As a result, the optimum solution could be quickly found so that the number of trials is substantially dropped, thus computational cost is considerably saved. In the next section, we will perform thinned array synthesis using MIFT for various linear arrays.

3. NUMERICAL RESULTS

We first considered demonstrating the difference between IFT and MIFT. Suppose a 200-element thinned array with the object fill factor $f_0 = 50\%$. The initial element distributions of the two methods within the same trial should be identical before performing the comparison. Then we performed ten independent trials of IFT and MIFT and arbitrarily chose the synthesis result of one single trial to illustrate the difference as shown in Figure 1.

Figures 1(a) and (b) respectively depict the normalized far field patterns produced by IFT and MIFT. The maximum sidelobe level (MSLL) obtained by MIFT is $-19.01\,\mathrm{dB}$, $1.96\,\mathrm{dB}$ lower than that obtained by IFT. Moreover, the sidelobe region of the far field pattern has intense oscillation, and the sidelobes of some points may rise abnormally in IFT, whereas in MIFT, the phenomenon was excellently restrained in a relative low level. Similar conclusions could also be obtained through all the other trials.

Then, to further demonstrate the effectiveness of MIFT, we consider applying MIFT to various linear arrays for the purpose of getting lower SLL as well as an appropriate beamwidth. The element spacing is half wavelength, and the coupling effect between the array elements is neglected. The number of sampling point of FFT is equal

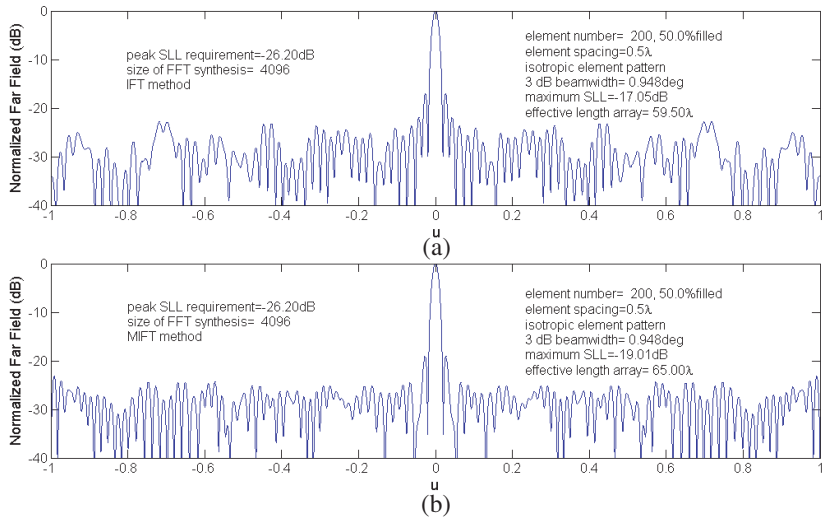

Figure 1. Normalized far-field pattern for a 200-element thinned array with 50% fill factor. (a) IFT method. (b) MIFT method.

to 4096 for all the illustrations except the third case. In addition, all the synthesis results are compared with the published reports [31, 33].

3.1. Symmetrical Thinned Array

A 200-element array, symmetric about its centre, is considered in the first case and has an object fill factor f_0 of 77%, RPSL of -24.80 dB. The initial fill factor $f_I = 0.99$, the step size $\alpha = 0.01$ so that two symmetrical elements could be truncated in each iteration cycle. The fill factor f could be expressed by the equation

$$f = f_I - \alpha * T \quad f \geq f_0 \tag{4}$$

where T (the value is 0, 1, 2, ...) represents the number of iterations.

Figure 2 shows the synthesis result of 30 independent trials. For convenience, in this paper, the pattern which has the minimum MSLL among 30 trials is chosen as the optimum pattern that we expected. This minimum MSLL is defined as the optimum sidelobe level (OSL). Figure 2(a) depicts the normalized far field pattern of the optimum element distributions among 30 trials featuring an OSL of -23.03 dB, which is lower than the reported value of -22.92 dB [33].

The score of 30 trials is shown by the histogram in Figure 2(b) that presents the frequency distribution of the MSLL performance of the 30 thinned element distributions. It can be noted that all

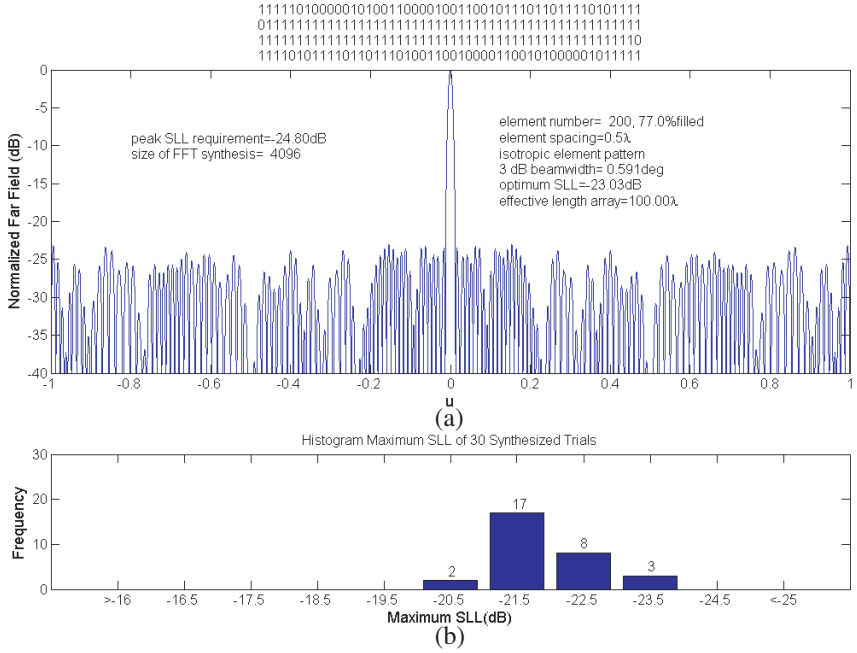

Figure 2. A 200-element symmetrical thinned array with 77% fill factor. (a) The far-field pattern with optimum SLL among 30 trials. (b) MSLL distribution of 30 independent trials.

the element distributions have a MSLL below -20 dB; 28 element distributions have a MSLL below -21 dB; 11 element distributions have a MSLL below -22 dB. If we normalize these various numbers of element distributions by the total population and express them in terms of the percentage, they are 100%, 93.33%, and 36.67% of the total population, whereas the corresponding percentages by IFT are 45.7%, 13.53%, and 0.58% [33]. It can be seen that the result yielded by MIFT has obviously high percentage of element distributions with low MSLL than the result produced by IFT. It is a good demonstration of the effectiveness of the proposed method.

Therefore, in MIFT, the bad solutions are massively excluded so that only a small number of trials, corresponding to a small number of iterations, is needed to reach the optimum solution. In this illustration, each trial contains 23 iterations, which means $\gamma = 23$, so the total number of iterations among 30 trials is 690. However, in the published report, by IFT, 10000 trials are needed. If we assume that there are 7 iterations (may be more) in each trial, then

the total number of iterations is 7×10^4. We can see that MIFT method needs approximately 1% of the iterations that IFT needs. So the computational time is substantially dropped. It takes about 2.05 seconds by MIFT, whereas IFT needs about 120 seconds [33].

The binary string on the top of Figure 2(a) describes the distribution of array elements state, where the value one represents the state 'turned on', and the value zero represents the state 'turned off'. The top line of the binary string represents the state of 1–50 elements, and the second, third and fourth lines represent the states of 51–100, 101–150, and 151–200 elements, respectively. Similarly, the binary strings in the following illustrations have the same meaning.

In the second test case, MIFT is applied to the same antenna array but with the object fill factor f_0 of 66%, RPSL -24.55 dB. Figure 3 shows the synthesis result of 30 independent trials. The obtained OSL is -22.84 dB, and the 3 dB beamwidth is 0.685 degree, which are almost as well as those by IFT in the published report [33]. The histogram in

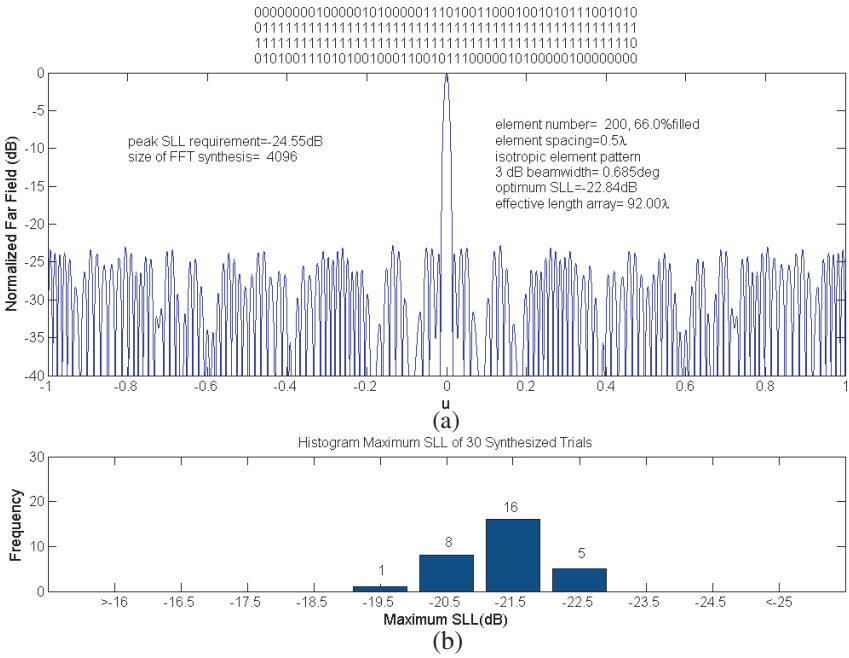

Figure 3. A 200-element symmetrical thinned array with 66% fill factor. (a) The far-field pattern with optimum SLL among 30 trials. (b) MSLL distribution of 30 independent trials.

Figure 3(b) shows that 29, 21, 5 element distributions have the MSLL respectively below $-20\,\mathrm{dB}$, $-21\,\mathrm{dB}$ and $-22\,\mathrm{dB}$, that are 96.67%, 70% and 16.67% of the total population, while the corresponding percentages by IFT are 58.54%, 17.08% and 0.91% [33]. It is also demonstrated that the result produced by MIFT has an obviously high percentage of element distributions with low MSLL than the result yielded by IFT. In other words, the bad solutions are largely excluded through MIFT.

Similarly, in each trial of the case, $\gamma = 34$, so the total number of iterations among 30 trials is 1020, and the value is also far less than the total number of iterations that IFT needed. Therefore, to get the optimum solution, only 3.2 seconds are consumed by this method while IFT needs about 120 seconds [33].

The convergence curves of MSLL of Figure 2 versus the various magnitudes of fill factors are depicted in Figure 4: the blue curve represents the best trial #11 with minimum MSLL of $-23.03\,\mathrm{dB}$; the black curve represents the worst trial #14 with minimum MSLL of $-20.81\,\mathrm{dB}$. To demonstrate the robustness of MIFT, we further calculate the variation of average MSLL among 30 trials versus different fill factors as the red curve shown in Figure 4. It could be seen that with the decrement of the fill factor, the average MSLL is gradually dropped and converged to a value near the OSL. So the average MSLL has good convergence features.

Similarly, Figure 5 shows the convergence curves of MSLL of Figure 3 versus different fill factors: the best trial #24 with minimum MSLL of $-22.84\,\mathrm{dB}$ and the worst trial #27 with minimum MSLL

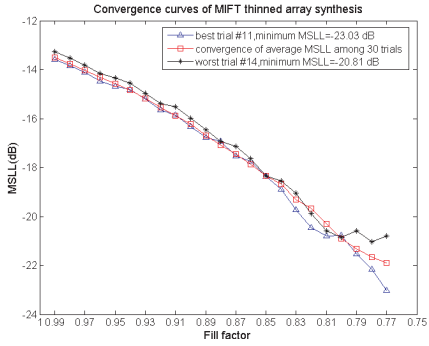

Figure 4. Convergence curves of the maximum SLL during the MIFT thinning synthesis of Figure 2.

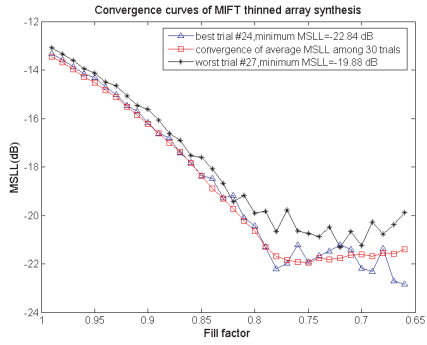

Figure 5. Convergence curves of the maximum SLL during the MIFT thinning synthesis of Figure 3.

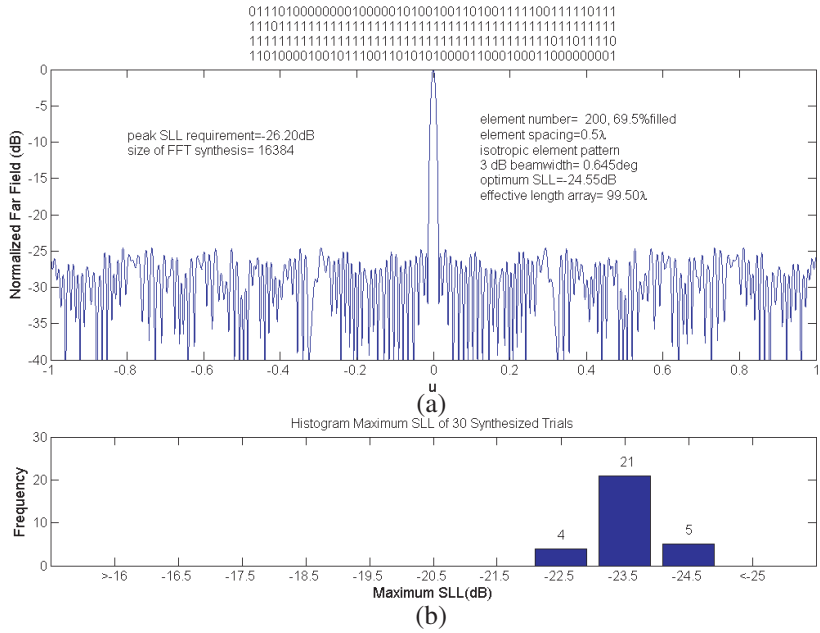

Figure 6. A 200-element asymmetrical thinned array with 69.5% fill factor. (a) The far-field pattern with optimum SLL among 30 trials. (b) MSLL distribution for 30 independent trials.

of −19.88 dB. The average MSLL among 30 trials also has good convergence features.

3.2. Asymmetrical Thinned Array

A 200-element asymmetrical array with f_0 of 69.5% and RPSL of −26.20 dB is considered in the third case. The initial fill factor $f_I = 0.995$, the step size $\alpha = 0.005$ so that one array element could be truncated in each iteration cycle. The synthesis result is shown in Figure 6.

The optimum thinned array element distributions shown in Figure 6(a) produce a far field pattern with an OSL of −24.55 dB, which is 0.25 dB lower than that by IFT in the literature report and with 3 dB beamwidth almost invariable [33]. The total number of iterations in this case is 1830. The computational time is 21 seconds by MIFT, which is about one seventeenth of the time consumed by IFT [33]. The sampling point K is raised to 16384 in this case to get the lowest SLL value.

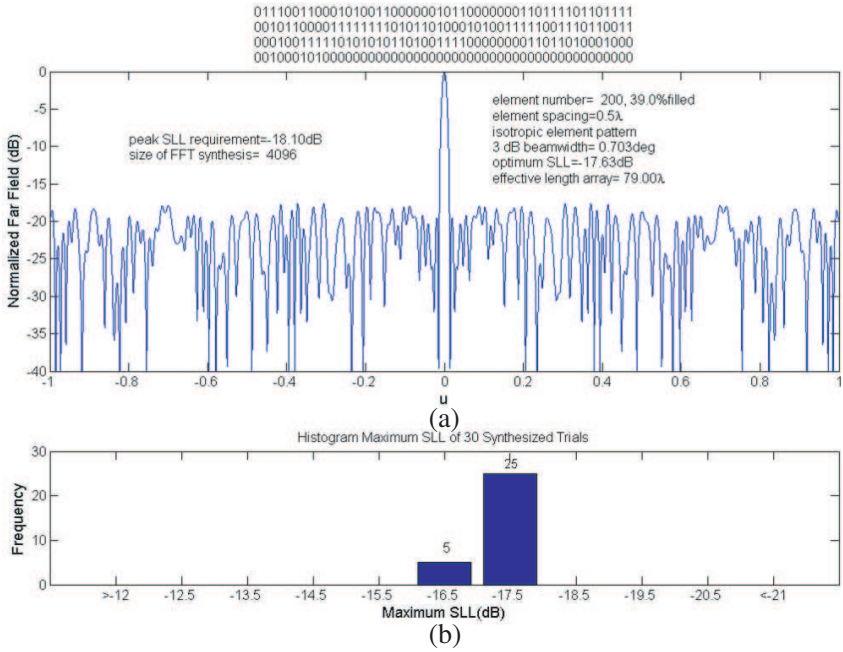

Figure 7. A 200-element asymmetrical thinned array with 39% fill factor. (a) The far-field pattern with optimum SLL among 30 trials. (b) MSLL distribution for 30 independent trials.

Applying MIFT to a massively thinned array with f_0 of 39% and RPSL of -18.10 dB is considered in the fourth case. The obtained result, as depicted in Figure 7, has an OSL of -17.63 dB, but the 3 dB beamwidth η is 0.703 degree, which is obviously broadened than 0.546 degree in the published report [33], so it is not a desired solution. To get a solution featuring low SLL and narrow beam simultaneously, the MIFT will be further modified in Section 3.4.

Similar to the foregoing cases, Figures 8 and 9 respectively depict the convergence curves of MSLL in Figures 6 and 7. The curves also fully demonstrate the good convergence features of MSLL. Table 1 shows the comparative results of the above four illustrations produced by MIFT and IFT.

3.3. The Influence of Sampling Point

The sampling point K is an important parameter in DFT. According to the theory of frequency-domain sampling [38], to reconstruct the array factor AF without aliasing, K should satisfy the relationship $K \geq M$,

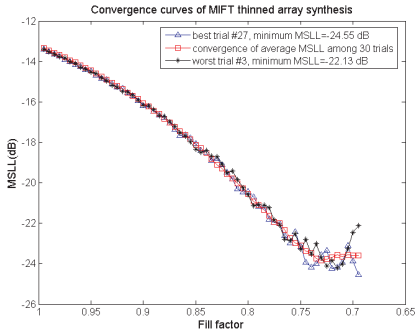

Figure 8. Convergence curves of the maximum SLL during the MIFT thinning synthesis of Figure 6.

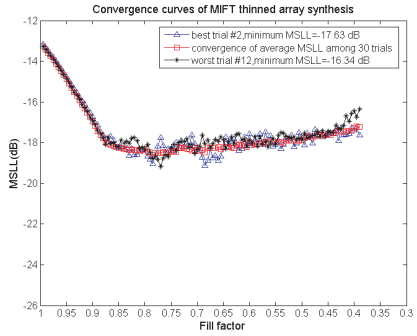

Figure 9. Convergence curves of the maximum SLL during the MIFT thinning synthesis of Figure 7.

Table 1. The comparative results of the four illustrations produced by MIFT and IFT.

Fill factor (%)	Optimum SLL (dB)		3 dB Beamwidth η (degree)		time consumed (second)		Effective length $L\,(\lambda)$	
	MIFT	IFT[33]	MIFT	IFT[33]	MIFT	IFT[33]	MIFT	IFT[33]
77	−23.03	−22.92	0.591	0.588	2.05	120	100	100
66	−22.84	−22.86	0.685	0.685	3.20	120	92	93
69.5	−24.55	−24.30	0.645	0.643	21.0	360	99.5	99
39	−17.63	−17.33	0.703	0.546	11.90	180	79	95.5

where M represents the size of the array. So for a 200-element position array, K should be no less than 200. Furthermore, if we wish to have a better picture that could provide sufficient details of AF, it could be realized by means of zero padding.

However, in both MIFT and IFT, the amount of zero padding obviously influences synthesis result. If zero padding is not enough, the low resolution may make some points of AF lost, and these points may have high sidelobe levels. If zero padding is excessive, the high resolution will make more points with their SLL exceeding RPSL in the sidelobe region. Accordingly, more points with their SLL have to be lowered to adapt to the sidelobe threshold during performing IFT or MIFT and thereby considerably change AF, which will in turn change the MSLL of the renewed AF after performing IFT or MIFT, and we cannot ensure whether the MSLL of the renewed AF is improved or

Table 2. The optimum results of above four illustrations produced by MIFT for various sampling points.

Fill factor (%)	77 (case 1)		66 (case 2)		69.5 (case 3)		39 (case 4)	
Sampling point	OSL (dB)	η (deg)	OSL (dB)	η (deg)	OSL (dB)	η (deg)	OSL (dB)	η (deg)
1024	−22.97	0.588	−22.29	0.671	−24.38	0.643	−17.43	0.643
2048	−22.83	0.588	−22.59	0.699	−24.33	0.650	−17.67	0.713
3072	−23.03	0.592	−22.36	0.690	−24.25	0.643	−17.68	0.835
4096	−23.03	0.591	−22.84	0.685	−24.39	0.650	−17.63	0.703
8192	−22.92	0.575	−22.07	0.692	−24.57	0.649	−17.85	0.860
16384	−22.88	0.590	−22.53	0.692	−24.55	0.645	−17.70	0.761

deteriorated.

To explore how the different sampling points influence the synthesis result, based on the illustrations in Sections 3.1, 3.2, we further perform array thinning using MIFT with various sampling points. The obtained results are shown in Table 2.

From Table 2, we can see that K has random influences on the synthesis result. Generally, we consider an appropriate K corresponding to the value which yields the lowest SLL as well as narrow beam. Thus we can see from Table 2 that the best value of K for the third case is 8192 or 16384, but 4096 for the other cases.

Nevertheless, although the possible optimum result may be obtained by a low sampling point, it may be just an illusion because of low resolution. For example, in case 1, when $K = 1024$, the obtained optimum element distributions among 30 trials produce a far field pattern with OSL of -22.97 dB and 3 dB beamwidth 0.588 degree. Although the result seemingly satisfies our requirement, when we further calculate AF based on this optimum element distributions by more zero padding with $K = 4096$ and 16384, both the obtained AF have OSL of -22.85 dB, which is about 0.12 dB higher than the value when $K = 1024$, so we regard 1024 as an improper sampling point.

Therefore, we suppose two steps that help us to select the size of K. The first step is to select the value which could produce the lowest SLL with a little compromise of beamwidth. The second step is based on the selected K and the corresponding element distributions in the first step. We further calculate AF by more zero padding with sampling point such as $4K$, $16K$ to get the detailed information of AF. If the MSLL of the renewed AF is almost invariable, we regard K as

the most suited sampling point, or else we have to reselect K trial and error according to the two steps just related above.

3.4. Further Modification

In most cases, lower SLL can be obtained only at the price of widening mainlobe. One purpose of the array synthesis is to make a compromise between low SLL and narrow beam. In addition, as related above, although MIFT has been successfully used for moderately truncated arrays, it suffers from beam broadening when the array elements are massively truncated. In this section, MIFT is further modified in order to maintain low SLL but with a little sacrifice of beamwidth.

Suppose an arbitrary normalized far field pattern as shown in Figure 10. The symbols of triangle in the figure represent the sampling points in the sidelobe region, while the symbols of asterisk represent the sampling points in the mainlobe region. The points A, B, C, D, E, F, G, etc., represent the successive sampling points in the left mainlobe region with point A the first null of the left mainlobe. Accordingly, the mirror points, $A1$, $B1$, $C1$, $D1$, $E1$, $F1$, $G1$, represent the successive sampling points in the right mainlobe region with point $A1$ the first null, too.

Furthermore, in Figure 10, we suppose that the upper doted line represents the requirement peak SLL and that the bottom dotted line represents the specified SLL which is lower than RPSL. In both IFT and MIFT, if there are some points in sidelobe region with their SLL above RPSL, we will forcefully lower their SLL to one constant value named specified SLL. The SLL values of the sampling points in mainlobe region are unchanged even though they may violate the

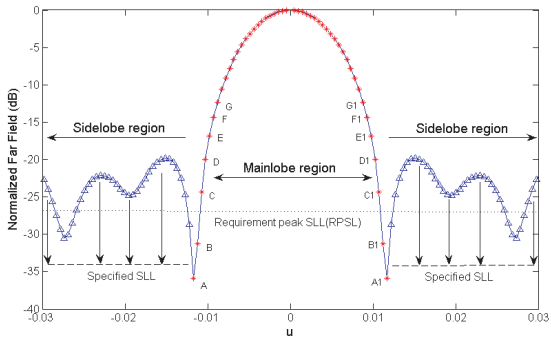

Figure 10. An arbitrary normalized far field pattern to illustrate the modified MIFT.

sidelobe threshold. Nevertheless, in the modified MIFT, in addition to the above operations, we successively choose Q sampling points located at the edge of the mainlobe region and then, forcefully make the SLLs of these points lower than their actual values. In detail, we suppose $Q = 4$, then the sampling points A, B and their mirror points $A1$, $B1$ are chosen as those to be lowered. This operation could be easily realized through adding only a few lines of MATLAB code to MIFT.

For example, if we assume that the initial sidelobe levels of points A, B and $A1$, $B1$ are $-35.9\,\text{dB}$, $-31.3\,\text{dB}$, $-35.5\,\text{dB}$, and $-31.2\,\text{dB}$, respectively, the variation value $\beta = -20\,\text{dB}$, then the corrected SLL values of A, B, $A1$, $B1$ are $-55.9\,\text{dB}$, $-51.3\,\text{dB}$ and $-55.5\,\text{dB}$, $-51.2\,\text{dB}$.

Figure 11 shows the synthesis result using modified MIFT for a 200-element asymmetrical array with f_0 of 39%, where we set $Q = 12$, $\beta = -20\,\text{dB}$. The obtained OSL is $-17.24\,\text{dB}$ with $3\,\text{dB}$ beamwidth 0.549 degree. The result is almost as good as that produced by IFT [33]. However, the time cost is only 11 seconds, about one sixteenth of the time consumed by IFT [33]. Furthermore, if we set $Q = 16$ with β invariable, the obtained optimum far field pattern has OSL of $-16.85\,\text{dB}$ and η of 0.528 degree.

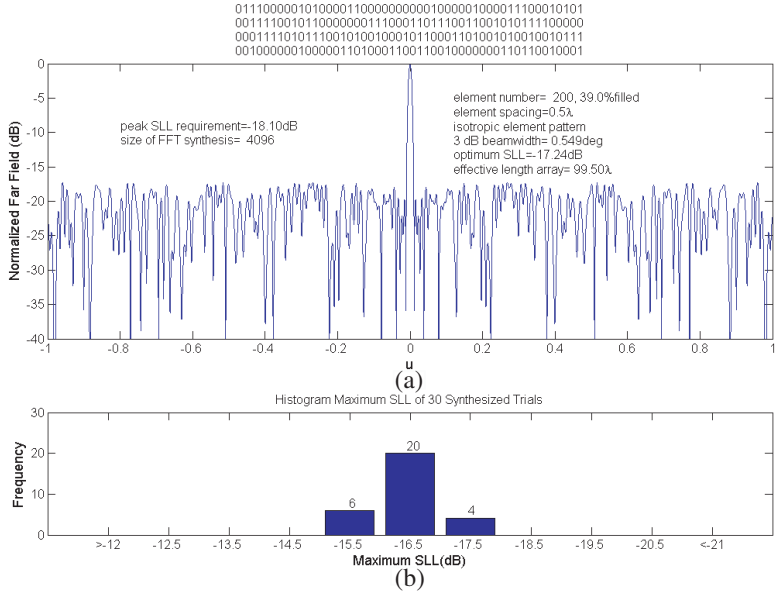

Figure 11. A 200-element asymmetrical thinned array with 39% fill factor. (a) The far-field pattern with optimum SLL among 30 trials. (b) MSLL distribution for 30 independent trials.

More trials show that β has less important influences on the synthesis result than Q does. So β could be treated as a constant value in modified MIFT. Table 3 shows the synthesis results of the same array using the modified MIFT among various Q values, where $\beta = -20\,\text{dB}$. We can see that through modulating the magnitude of parameter Q, we could efficiently obtain a possible optimum solution with low SLL as well as narrow beam.

3.5. Comparing with Other Optimum Algorithms

To further demonstrate the robustness of MIFT, in this section, we compare the array synthesis results by MIFT with those by GA and ACO in the published reports [31, 32].

We consider a linear array of 100 isotropic antennas symmetrically spaced 0.5λ apart along x-axis with its center at the origin. Then MIFT is performed to thin this antenna array in three cases: 1) 20% thinning; 2) 22% thinning; 3) 24% thinning.

Table 3. The synthesis results using modified MIFT among various Q values.

Q	Optimum SLL (dB)	3 dB Beamwidth η (degree)	Effective length (λ)
6	−17.15	0.601	94
12	−17.24	0.549	99.5
16	−16.85	0.528	100
30	−16.4	0.504	100

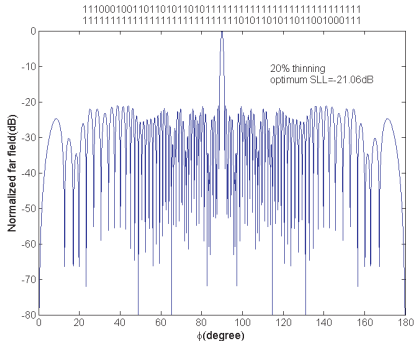

Figure 12. The normalized far field pattern of a 100-element symmetrical array that was 20% thinned by MIFT.

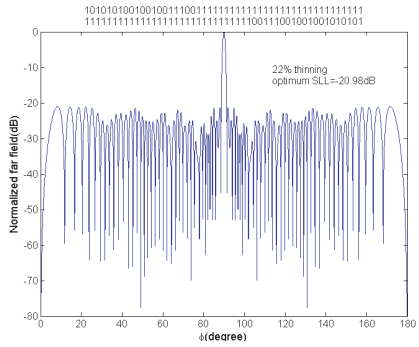

Figure 13. The normalized far field pattern of a 100-element symmetrical array that was 22% thinned by MIFT.

Table 4. Comparative results produced by MIFT, GA, and ACO.

Percentage of thinning (%)	MIFT			GA [31]	ACO [32]
	SLL (dB)	3 dB beamwidth (degree)	time consumed (second)	SLL (dB)	SLL (dB)
20	−21.06	1.154	1.1	/	−20.52
22	−20.98	1.193	1.1	−20.56	/
24	−20.53	1.22	1.2	−20.53	/

Table 5. Turned off element numbers by MIFT for all cases.

Percentage of thinning (%)	Turned off element numbers
20	±29, ±31, ±34, ±36, ±39, ±42, ±43, ±45, ±46, ±47
22	±31, ±32, ±36, ±37, ±39, ±40, ±42, ±43, ±45, ±47, ±49
24	±29, ±30, ±34, ±36, ±38, ±40, ±41, ±43, ±44, ±46, ±49, ±50

Figure 12 shows the optimum far field pattern of the 20% thinned array produced by MIFT among 30 trials, where ϕ is the azimuth angle of the far field point measured from x-axis.

The obtained optimum SLL is −21.06 dB, which is lower than the SLL of −20.52 dB that is obtained by ACO [32]. Similarly, Figure 13 shows the far field pattern of the same array but 22% thinned, the obtained optimum SLL is −20.98 dB, which is about 0.42 dB lower than GA result [31].

Table 4 shows the comparative results produced by MIFT, GA and ACO. Table 5 shows the turned off element numbers by MIFT for all cases. All the results are obtained by a PC equipped with an Intel Pentium Dual core E5200 Processor running at 2.5 GHz provided with 2 GB RAM.

4. CONCLUSION

The synthesis results by MIFT show a good agreement between the desired and synthesized specifications for all above cases with high efficiency. So it is an effective method for thinning uniformly excited

array. Furthermore, when we compare IFT with MIFT, it can be found that in MIFT, bad solutions are excluded in maximum extent through gradual thinning ways so that the optimum solution can be reached by only a small number of trials. Therefore, plenty of the iterations and thereby plenty of computational time are saved. Nevertheless, the method can save computer time only for small or medium size array. For a large array containing plenty of elements, the time consumed by MIFT would be much more than the time needed by IFT. For example, if we suppose that a uniformly excited planar array contains 5000 element positions, if the object fill factor $f_0 = 50\%$, the total number of trials is 30, then the total number of iterations by MIFT is about 7.5×10^4. However, when it comes to IFT, we assume that 1000 trials are included and that each trial contains 10 iteration cycles, the total number of iterations will be 1×10^4, which is only about one seventh of the total iterations needed by MIFT.

However, because IFT is apt to fall into local solutions, whereas MIFT provides a good way to avoid trapping, thus for a large array, the optimum solution for thinned array synthesis may be obtained by combining the two methods together.

ACKNOWLEDGMENT

The authors would like to thank the anonymous reviewers for providing a number of very important comments and suggestions, which have significantly improved this paper.

REFERENCES

1. Ayestarán, R. G., J. Laviada, and F. Las-Heras, "Realistic antenna array synthesis in complex environments using a mom-svr approach," *Journal of Electromagnetic Waves and Applications*, Vol. 23, No. 1, 97–108, 2009.
2. Orchard, H. J., R. S. Elliott, and G. J. Stern, "Optimising the synthesis of shaped beam antenna patterns," *IEE Proceedings*, Vol. 132, No. 1, 63–68, 1985.
3. Franceschetti, G., G. Mazzarella, and G. Panariello, "Array synthesis with excitation constraints," *IEE Proceedings*, Vol. 135, No. 6, 400–407, 1988.
4. Wang, W.-B., Q. Y. Feng, and D. Liu, "Application of chaotic particle swarm optimization algorithm to pattern synthesis of antenna arrays," *Progress In Electromagnetics Research*, Vol. 115, 173–189, 2011.

5. Liu, D., Q. Y. Feng, W.-B. Wang, and X. Yu, "Synthesis of unequally spaced antenna arrays by using inheritance learning particle swarm optimization," *Progress In Electromagnetics Research*, Vol. 118, 205–221, 2011.
6. Zaharis, Z. D. and T. V. Yioultsis, "A novel adaptive beamforming technique applied on linear antenna arrays using adaptive mutated boolean PSO," *Progress In Electromagnetics Research*, Vol. 117, 165–179, 2011.
7. Carro Ceballos, P. L., J. de. Mingo Sanz, P. G. Dúcar, "Radiation pattern synthesis for maximum mean effective gain with spherical wave expansions and particle swarm techniques," *Progress In Electromagnetics Research*, Vol. 103, 355–370, 2010.
8. Zaharis, Z. D., S. K. Goudos, and T. V. Yioultsis, "Application of Boolean PSO with adaptive velocity mutation to the design of optimal linear antenna arrays excited by uniformamplitude current distribution," *Journal of Electromagnetic Waves and Applications*, Vol. 25, No. 10, 1422–1436, 2011.
9. Khodier, M. M. and C. G. Christodoulou, "Linear array geometry synthesis with minimum sidelobe level and null control using particle swarm optimization," *IEEE Trans. on Antennas and Propag.*, Vol. 53, No. 8, 2674–2679, 2005.
10. Lanz Diego, M., J. R. Pérez Lopez, and J. Basterrechea, "Synthesis of planar arrays using a modified particle swarm optimization algorithm by introducing a selection operator and elitism," *Progress In Electromagnetics Research*, Vol. 93, 145–160, 2009.
11. Li, W.-T., X.-W. Shi, and Y.-Q. Hei, "An improved particle swarm optimization algorithm for pattern synthesis of phased arrays," *Progress In Electromagnetics Research*, Vol. 82, 319–332, 2008.
12. Mahanti, G. K., A. Chakrabarty, and S. Das, "Phase-only and amplitude phase synthesis of dual-pattern linear antenna arrays using floating-point genetic algorithms," *Progress In Electromagnetics Research*, Vol. 68, 247–259, 2007.
13. Chen, K. S., Z. S. He, and C. L. Han, "A modified real GA for the sparse linear array synthesis with multiple constraints," *IEEE Trans. on Antennas and Propag.*, Vol. 54, No. 7, 2169–2173, 2006.
14. Li, F., Y.-C. Jiao, L.-S. Ren, Y.-Y. Chen, and L. Zhang, "Pattern synthesis of concentric ring array antennas by differential evolution algorithm," *Journal of Electromagnetic Waves and Applications*, Vol. 25, No. 2–3, 421–430, 2011.
15. Mallipeddi, R., J. P. Lie, P. N. Suganthan, S. G. Razul, and C. M. S. See, "A differential evolution approach for robust

adaptive beamforming based on joint estimation of look direction and array geometry," *Progress In Electromagnetics Research*, Vol. 119, 381–394, 2011.

16. Li, R., L. Xu, X.-W. Shi, N. Zhang, and Z.-Q. Lv, "Improved differential evolution strategy for antenna array pattern synthesis problems," *Progress In Electromagnetics Research*, Vol. 113, 429–441, 2011.
17. Rodriguez, J. A., F. Ares, and E. Moreno, "Linear array pattern synthesis optimizing array element excitations using the simulated annealing technique," *Microwave Opt. Technol. Lett.*, Vol. 23, No. 4, 224–226, 1999.
18. Caorsi, S., A. Lommi, et al., "Peak sidelobe level reduction with a hybrid approach based on GAs and difference sets," *IEEE Trans. on Antennas and Propag.*, Vol. 52, No. 4, 1116–1121, 2004.
19. Pérez Lopez, J. R. and J. Basterrechea, "Hybrid particle swarm-based algorithms and their application to linear array synthesis," *Progress In Electromagnetics Research*, Vol. 90, 63–74, 2009.
20. Donelli, M., S. Caorsi, et al., "Linear antenna synthesis with a hybrid genetic algorithm," *Progress In Electromagnetics Research*, Vol. 49, 1–22, 2004.
21. Rajo-Iglesias, E. and Ó. Quevedo-Teruel, "Linear array synthesis using an ant colony optimization based algorithm," *IEEE Antennas and Propagation Magazine*, Vol. 49, No. 2, 70–79, 2007.
22. Liu, Y., Z.-P. Nie, and Q. H. Liu, "A new method for the synthesis of non-uniform linear arrays with shaped power patterns," *Progress In Electromagnetics Research*, Vol. 107, 349–363, 2010.
23. Dib, N. I., S. K. Goudos, and H. Muhsen, "Application of taguchi's optimization method and self-adaptive differential evolution to the synthesis of linear antenna arrays," *Progress In Electromagnetics Research*, Vol. 102, 159–180, 2010.
24. Li, G., S. Yang, M. huang, and Z. Nie, "Sidelobe suppression in time modulated linear arrays with unequal element spacing," *Journal of Electromagnetic Waves and Applications*, Vol. 24, Nos. 5–6, 775–783, 2010.
25. Fondevila, J., J. C. Brégains, et al., "Optimizing uniformly excited linear arrays through time modulation," *IEEE Antennas and Wireless Propag. Lett.*, Vol. 3, 298–301, 2004.
26. Haupt, R. L., "Thinned arrays using genetic algorithms," *IEEE Trans.on Antennas and Propag.*, Vol. 42, No. 7, 993–999, 1994.
27. Fernández-Delgado, M., J. A. Rodríguez-González, R. Iglesias,

S. Barro, and F. J. Ares-Pena, "Fast array thinning using global optimization methods," *Journal of Electromagnetic Waves and Applications*, Vol. 24, No. 16, 2259–2271, 2010.

28. Wang, J., B. Yang, S. H. Wu, and J. Chen, "A novel binary particle swarm optimization with feedback for synthesizing thinned planar arrays," *Journal of Electromagnetic Waves and Applications*, Vol. 25, No. 14–15, 1985–1998, 2011.
29. Bucci, O. M., T. Isernia, and A. F. Morabito, "A deterministic approach to the synthesis of pencil beams through planar thinned arrays," *Progress In Electromagnetics Research*, Vol. 101, 217–230, 2010.
30. Jin, N. and Y. Rahmat-Samii, "Advances in particle swarm optimization for antenna designs: Real-number, binary, single-objective and multi-objective implementations," *IEEE Trans. on Antennas and Propag.*, Vol. 55, No. 3, 556–567, 2007.
31. Mahanti, G. K., N. N. Pathak, and P. K. Mahanti, "Synthesis of thinned linear antenna arrays with fixed sidelobe level using real-coded genetic algorithm," *Progress In Electromagnetics Research*, Vol. 75, 319–328, 2007.
32. Quevedo-Teruel, Ó. and E. Rajo-Iglesias, "Ant colony optimization in thinned array synthesis with minimum sidelobe level," *IEEE Antennas and Wireless Propag. Lett.*, Vol. 5, 349–352, 2006.
33. Keizer, W. P. M. N., "Linear array thinning using iterative FFT techniques," *IEEE Trans. on Antennas and Propag.*, Vol. 56, No. 8, 2757–2760, 2008.
34. Keizer, W. P. M. N., "Element failure correction for a large monopulse phased array antenna with active amplitude weighting," *IEEE Trans. on Antennas and Propag.*, Vol. 55, No. 8, 2211–2218, 2007.
35. Keizer, W. P. M. N., "Low sidelobe patterns synthesis using iterative fourier techniques coded in MATLAB," *IEEE Antennas and Propagation Magazine*, Vol. 51, No. 2, 137–150, 2009.
36. Bucci, O. M., G. D'Elia, G. Mazzarella, and G. Panariello, "Antenna pattern synthesis: A new general approach," *Proceedings of the IEEE*, Vol. 82, No. 3, 358–371, 1994.
37. Quijano, J. L. A. and G. Vecchi, "Alternating adaptive projections in antenna synthesis," *IEEE Trans. on Antennas and Propag.*, Vol. 58, No. 3, 727–737, 2010.
38. Proakis, J. G. and D. G. Manolakis, *Digital Signal Processing Principles, Algorithms, and Applications*, 4th edition, 449–459, Publishing House of Electronics Industry, Beijing, 2007.